Activation and Propagation of Tumor-infiltrating Lymphocytes on Clinical-grade Designer Artificial Antigen-presenting Cells for Adoptive Immunotherapy of Melanoma

Marie-Andrée Forget,† Shruti Malu,* Hui Liu,‡ Christopher Toth,* Sourindra Maiti,† Charuta Kale,* Cara Haymaker,* Chantale Bernatchez,* Helen Huls,† Ena Wang,‡§ Francesco M. Marincola,§ Patrick Hwu,* Laurence J.N. Cooper,† and Laszlo G. Radvanyi*‖*

Purpose: Adoptive cell therapy with autologous tumor-infiltrating lymphocytes (TIL) is a therapy for metastatic melanoma with response rates of up to 50%. However, the generation of the TIL transfer product is challenging, requiring pooled allogeneic normal donor peripheral blood mononuclear cells (PBMC) used in vitro as "feeders" to support a rapid-expansion protocol. Here, we optimized a platform to propagate TIL to a clinical scale using K562 cells genetically modified to express costimulatory molecules such as CD86, CD137-ligand, and membrane-bound IL-15 to function as artificial antigen-presenting cells (aAPC) as an alternative to using PBMC feeders.

Experimental Design: We used aAPC or γ-irradiated PBMC feeders to propagate TIL and measured rates of expansion. The activation and differentiation state was evaluated by flow cytometry and differential gene expression analyses. Clonal diversity was assessed on the basis of the pattern of T-cell receptor usage. T-cell effector function was measured by evaluation of cytotoxic granule content and killing of target cells.

Results: The aAPC propagated TIL at numbers equivalent to that found with PBMC feeders, whereas increasing the frequency of $CD8^+$ T-cell expansion with a comparable effector-memory phenotype. mRNA profiling revealed an upregulation of genes in the Wnt and stem-cell pathways with the aAPC. The aAPC platform did not skew clonal diversity, and $CD8^+$ T cells showed comparable antitumor function as those expanded with PBMC feeders.

Conclusions: TIL can be rapidly expanded with aAPC to clinical scale generating T cells with similar phenotypic and effector profiles as with PBMC feeders. These data support the clinical application of aAPC to manufacture TIL for the treatment of melanoma.

Received for publication July 9, 2014; accepted August 19, 2014.

From the *Department of Melanoma Medical Oncology; †Division of Pediatrics, MD Anderson Cancer Center, Houston, TX; ‡Infectious Disease and Immunogenetics Section, Department of Transfusion Medicine, Clinical Center and trans-NIH Center for Human Immunology, National Institutes of Health, Bethesda, MD; ‖Lion Biotechnologies, Woodland Hills, CA; and §Sidra Medical and Research Hospital, Doha, Qatar.

L.J.N.C. and L.G.R. are joint last-authors.

Reprints: Laszlo G. Radvanyi, Lion Biotechnologies, 21900 Burbank Blvd, 3rd floor, Woodland Hills, CA 91367. E-mail: laszlo.radvanyi@lionbio.com.

Supplemental Digital Content is available for this article. Direct URL citations appear in the printed text and are provided in the HTML and PDF versions of this article on the journal's Website, www.immunotherapy-journal.com.

Key Words: adoptive T-cell therapy, tumor-infiltrating lymphocytes, melanoma, artificial antigen-presenting cells, K562, costimulation

(*J Immunother* 2014;37:448–460)

Adoptive T-cell therapy (ACT) infusing propagated autologous tumor-infiltrating lymphocytes (TIL) ex vivo has been shown in multiple phase II clinical trials to be an effective investigational therapy for metastatic melanoma with sustained clinical response rates of approximately 50% according to RECIST criteria.[1–3] These antitumor effects are attributed to the infusion of T cells harvested from a tumor site that maintain a broad specificity during the tissue culture. Notably, the infusion of TIL has emerged to be a salvage therapy for some patients who progressed after multiple lines of prior therapy (including checkpoint blockade). The typical clinical protocol includes a lymphodepleting preconditioning regimen using cyclophosphamide and fludarabine, followed by coinfusion of TIL and IL-2.[2–4] Correlative biomarker studies on patients responding to this adoptive immunotherapy revealed attributes of the infusion product associated with therapeutic success. For example, an increased proportion of $CD8^+$ T cells and $CD8^+$ T cells expressing the B- and T-lymphocyte attenuator (BTLA) in the propagated TIL infusion product is associated with favorable outcomes.[3,5,6]

One obstacle limiting the distribution of TIL-based immunotherapy is the technical challenges associated with the manufacture of the autologous TIL-derived product. Currently, TIL expansion requires a 2-week rapid-expansion protocol (REP) using CD3 cross-linking and IL-2 after an initial expansion of TIL from small pieces of tumor (tumor fragments) with IL-2 alone.[7,8] This generates a final infusion product composed of 20–150 billion T cells.[7,8] A key component in the REP besides anti-CD3 and IL-2 is the presence of an excess of irradiated allogeneic peripheral blood mononuclear cells (PBMC) from healthy donors added as "feeder cells."[7,9] These feeders are needed to support TIL activation and propagation early during the REP. However, the procurement of large numbers of feeder cells (up to 10^{10} per patient treated) is difficult and expensive. The practicality of using these feeders is further compounded by the requirement to pool PBMC from multiple donors (4–6 donors at a time) to ensure optimal

activity, which introduces lot-to-lot heterogeneity and variability in activation of TIL. This problem is one of the key issues that has hindered the outscaling of TIL manufacturing and therapy.

A common bank of well defined, renewable, and designed feeders will remedy these issues associated with PBMC-derived feeders. Artificial antigen-presenting cells (aAPC) have been developed from K562 cells[10] and applied by our group for clinical expansion of genetically modified T cells from peripheral blood.[11–13] K562-derived aAPCs have been shown to expand bulk or antigen-specific T cells to large numbers while preserving clonal diversity.[11,14] K562 cells were genetically modified and cloned (designated clone 4) to homogenously express desired T-cell costimulatory molecules CD86, CD137-ligand (4-1BBL), high affinity Fc receptor (CD64) to allow antibody coating, and membrane-bound variant of IL-15 (mIL15, coexpressed with EGFP).[15] K562-based aAPC would be an appealing "off-the-shelf" feeder cell to expand TIL for human application. However, it is unclear whether aAPC will support a reproducible and scalable system for activation and propagation of human TIL and expansion yields comparable to or improved from the traditional REP needed for clinical application.

In this study, we investigated an alternative to PBMC feeders REP on the basis of activating and propagating melanoma TIL using aAPC in the traditional flask system and in a new "G-REX" culture flask system.[16] We found that the aAPC supports the rapid expansion of TIL to a similar extent as PBMC feeders with a comparable effector-memory phenotype, making aAPC suitable for GMP-grade melanoma TIL REP. We observed that the aAPC expansion platform was also able to favor the expansion of $CD8^+$ TIL, which we have found to be critical in mediating tumor regression in treated patients.[3] Our results show that aAPC may be used in lieu of PBMC to support the production of T cells from TIL for human application and, thus, we plan on retiring the traditional PBMC feeders from our approach to manufacturing clinical-grade T cells for melanoma.

MATERIALS AND METHODS

Initial Propagation of TIL From Human Melanoma Tumors

TILs used in this study were isolated from tumor samples obtained from melanoma patients with stages IIIc and IV disease undergoing surgery at the University of Texas MD Anderson Cancer Center (MDACC) according to Institutional Review Board–approved protocols and patient consent (LAB06-0755 and LAB06-0757). The initial TIL expansion was undertaken in 24-well plates from either small 3–5 mm^2 tumor fragments or after enzymatic digestion followed by centrifugation over a step gradient of 75% and 100% Ficoll, with the TIL collected from above the 100% Ficoll layer.[3,17] In both cases, the T cells were propagated for 3–5 weeks with 6000 IU/mL human recombinant IL-2 (Prometheus; San Diego, CA) in RPMI 1640 with Glutamax supplemented with 2 mM L-glutamine, 1 mM pyruvate, 1 × of HEPES, 50 μM 2-mercaptoethanol, 1 × Pen-Strep (Invitrogen, Carlsbad, CA), and 10% heat-inactivated human AB Serum (Sigma-Aldrich). Autologous tumor lines were established from enzymatically digested tumors by collecting the cells at the 75% Ficoll layer and used as targets.

Rapid Expansion of TIL (REP)

Cultured TILs were propagated by REP with anti-CD3 (OKT3; eBioscience, San Diego, CA) using pooled allogeneic irradiated PBMC feeder cells (ratio of 1 TIL to 200 feeders), which is identical to the protocol currently used for phase II clinical trials carried out at MDACC.[3] For TIL propagation carried out in the G-REX 100 M flask (Wilson-Wolf Manufacturing, New Brighton, MN), 5×10^6 TILs were seeded per G-REX flask on day 0 and the expansion was completed using same reagents, feeding schedule, and cell ratios as the current protocol performed in the traditional flask.

Rapid Expansion of TIL by aAPC

Cultured TILs were cocultured with irradiated aAPC [ratios ranging from 1:1 to 1:100 (TIL:aAPC)] that were derived from K562 cells genetically modified to coexpress CD19, CD64, CD86, CD137L, and mIL15 and cloned to obtain homogenous expression.[18] Before starting the REP, the K562 clone 4 aAPCs were irradiated at 150 Gy and preloaded with anti-CD3. Briefly, cells were incubated in X-VIVO 15 (LONZA, Walkersville, MD) media containing 0.2% of acetylcysteine (APP Pharmaceuticals, Schaumburg, IL) (at a concentration of 1 million/mL overnight), followed by an incubation with OKT3 (0.1–1 μg/mL) at 4°C for 30 minutes while rotating. Clone 4 aAPCs were then washed and frozen for subsequent usage. The TIL expansion in the G-REX 100 M using the aAPC was performed as previously described.

Flow Cytometry

Monitoring of clone 4 was done by staining with anti-CD64-PE, CD137L-PE, and CD86-APC (BD Bioscience, San Jose, CA) and OKT3 loading was evaluated by staining with a PE-conjugated AffiniPure $F(ab')_2$ fragment goat anti-mouse IgG (Jackson Immunology Research Laboratories, West Grove, PA). T cells were stained with anti-CD3-FITC (or PerCP-Cy5.5), CD8-PB (or APC-H7), CD16-PE, CD56-PE-Cy7 (or PE), CD27-APC, CD28-PE-Cy7, CD127-PE, BTLA-PE (clone J168), CD45RA-FITC (or V450), CD57-FITC (BD Bioscience), CD4-PerCP-Cy5.5, TIM3-APC (clone F38-2E2) (eBioscience), PD1-PerCP-Cy5.5 (clone EH12.2H7), and CCR7-PerCP-Cy5.5 (BioLegend, San Diego, CA). Cells were stained in 100 μL FACS buffer containing AQUA live/dead dye (Invitrogen) on ice for 30 minutes. For intracellular staining, cells were fixed and permeabilized using Cytofix/Cytoperm (BD Biosciences) and subsequently stained for granzyme B-PE, perforin-FITC (eBioscience), and in some cases also with cleaved caspase-3-PE (BD Biosciences). Data acquired using a FACScanto II cytometer (BD Biosciences) and analyzed using FlowJo v 7.6.5 (Treestar) with different subsets defined using size, viability, and "fluorescence minus one" (FMO) controls.

Direct TCR Expression Assay (DTEA)

Total RNA was isolated from post-REP TIL expanded with either feeders or aAPC using RNeasy Mini Kit (Qiagen, Germantown, MD), and quantified using a NanoDrop 1000 (Thermo Fisher Scientific, St Louis, MO). DTEA to measure the abundance of 45 Vα and 46 Vβ TCR chains was performed using the nCounter (model No. NCT-SYST-120) assay system (NanoString Technologies, Seattle, WA) as described.[19]

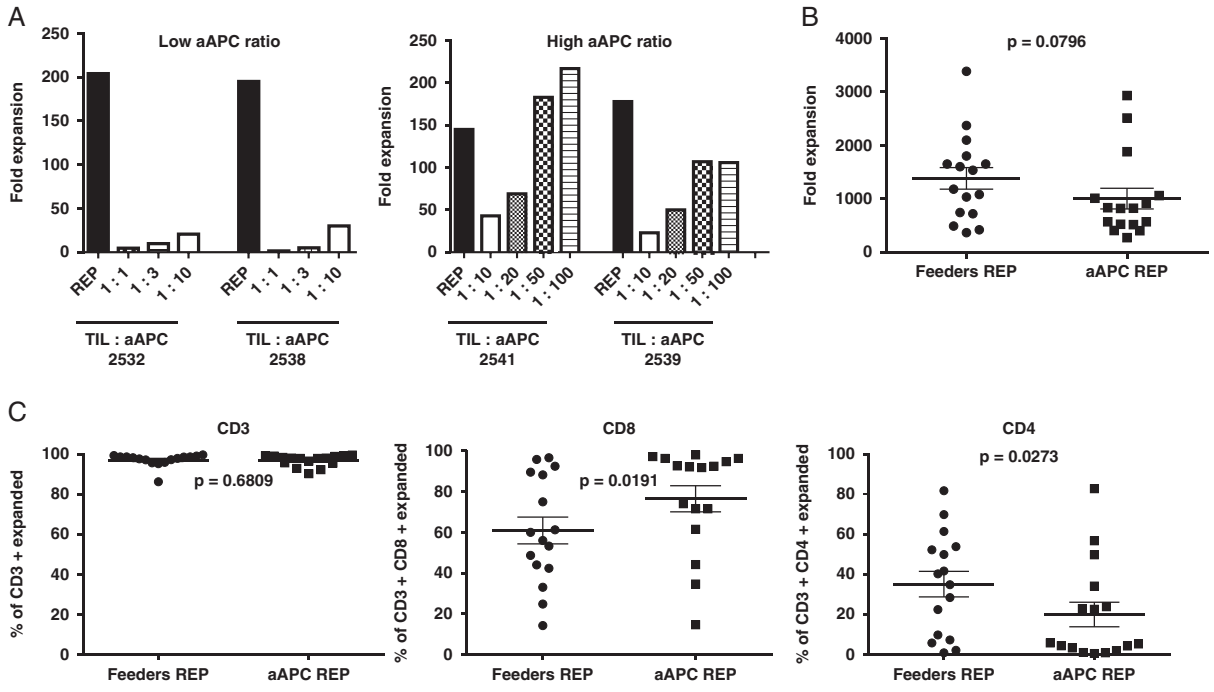

FIGURE 1. Rapid expansion of melanoma TIL using aAPC. A, Melanoma TILs cultured in high doses of IL-2 (6000 IU/mL) for 3–5 weeks were rapidly expanded using different TIL:aAPC ratios [low (1:1, 1:3, and 1:10) and high (1:10, 1:20, 1:50, and 1:100)] and 30 ng/mL of αCD3 mAb (OKT3) with IL-2. Fold expansion of bulk TIL was evaluated on day 7 of the REP. B, Graph showing cumulative data of fold expansion of bulk TIL lines. C, Percentage of $CD3^+$ TIL post-REP (left graph) obtained after 14 days of expansion. Middle and right graphs show post-REP frequency of, respectively, $CD3^+CD8^+$ and $CD3^+CD4^+$ TIL. For each TIL line, REPs were set up simultaneously using PBMC feeders (1:200) and aAPC (1:50) as an expansion platform for direct comparison. Statistics were determined using the paired *t* test, and a *P* value <0.05 was considered significant.

Gene Expression Analysis

Total RNA (300 ng) from T cells that completed propagation by REP or aAPC was amplified using Ambion WT expression kit (Life Technologies, Grand Island, NY) according to manufacturer's instructions. Briefly, mRNA was reverse transcribed into cDNA and a second strand cDNA was generated, which was then used as a template for in vitro transcription for cRNA synthesis. Following purification, the cRNA was converted into cDNA and excess RNA was removed by RNase H treatment. With the use of restriction digestion, cDNA was fragmented and labeled on the terminal end with the GeneChip WT Terminal Label kit (Affymetrix, Santa Clara, CA). The samples were hybridized to Human Gene ST 1.0 Arrays (Affymetrix) in a GeneChip Hybridization Oven 640 for >16 hours, at 45°C, 60 rpm, stained on a GeneChip Fluidics Station 450, and scanned by GeneChip Scanner 3000 7G (Affymetrix). Following quality control assessment, unprocessed data were engendered with Affymetrix GeneChip Command Console, and analyzed using Partek Genomic Suite 6.6 software after background subtraction and RMA normalization. Differentially expressed genes were defined by 2-way analysis of variance with $P < 0.005$. Genes were further analyzed for functional involvement and enrichment using ingenuity pathway analysis (Qiagen, Redwood City, CA).

T-cell–mediated Killing

Killing of HLA-A-matched melanoma tumor cells (target cells) by specific activated/propagated T cells was visualized by flow cytometry to measure the level of activated caspase-3 in target cells.[20] To test the class I dependency of killing, target cells were incubated for 3 hours at 37°C with 80 μg/mL of either MHC class I blocking antibody W6/32 or the IgG2a-matching isotype control (eBioscience).

IFN-γ Enzyme-linked Immunosorbent Assay (ELISA)

Antitumor reactivity of post-REP TIL was also tested by measuring IFN-γ secretion using ELISA on supernatants of cocultures of 5×10^4 TIL with 5×10^4 (triplicates) tumor cells from autologous or HLA-A-matched melanoma lines.[3] Assays were performed in 96-well plates and supernatants were collected after 16 hours and stored at −80°C until analysis. MHC class I blocking antibody W6/32 or the mouse IgG2a-matching isotype was also used as control in these assays, as previously described. TIL treated with PMA (50 pg/mL) and Ionomycin (2 μg/mL) were also included as a positive control. ELISA was performed using ELISA kits (Pierce, St Louis, MO).

RESULTS

Rapid Expansion of Melanoma TIL Using aAPC Leads to Similar Rates of TIL Expansion as PBMC Feeders and Favors $CD8^+$ T-cell Growth

The current REP used for the clinical manufacturing of melanoma TIL infusion products uses pooled irradiated PBMC as feeders and usually achieves TIL expansion in the range of 500- to 2000-fold over 14 days to generate infusion products used in TIL clinical trials. We first assessed

whether K562-aAPC (clone 4) loaded with OKT3 could achieve comparable levels of expansion from TIL, as the traditional PBMC feeders, but also preserve the $CD8^+$ T-cell component that has been shown to correlate with clinical response. Fig. S1, Supplemental Digital Content 1 (http://links.lww.com/JIT/A352) shows OKT3 loading as well as the expression levels of CD64, CD86, and 4-1BBL stably expressed in the clone 4 aAPC that were used in all the experiments. We first evaluated different ratios of aAPC added to TIL compared with the PBMC feeders REP to identify the best TIL:aAPC ratio yielding the highest and most consistent expansion. The most rapid phase of TIL cell division (population doublings) occurs during the first 7 days of the REP, reasoning that the initial 7-day period was enough to judge the activity of the aAPC. As shown in Figure 1A (left graph), lower ratios of TIL to aAPC (1:1 to 1:10) could not expand TIL to a similar level as the traditional REP with feeders (1:200 TIL:feeders). However, increased ratios of the aAPC increased the fold expansion, with a 1:50 ratio supporting near-maximal or maximal TIL expansion (Fig. 1A, right graph). On the basis of these data, we chose the 1:50 TIL:aAPC ratio for subsequent experiments and further development of this system.

Comparison of T Cells Propagated by PBMC Feeders REP and aAPC REP

The 1:50 TIL:aAPC ratio was used to activate and rapidly expand TIL for 14 days for a larger number of patient samples (n = 16). As shown in Figure 1B, there was no statistical difference ($P > 0.05$) in the fold expansion of TIL cocultured with aAPC versus propagated with PBMC feeders. After coculture the final TIL products were almost exclusively $CD3^+$ cells (Fig. 1C), but the aAPC REP yielded an increased percentage of $CD3^+CD8^+$ T cells with a concomitant decreased percentage of $CD3^+CD4^+$ T cells compared with traditional REP. The propagated products contained only a small frequency of NK cells (< 5%) as marked by $CD56^+$ or $CD56^+CD16^+$ cells (data not shown). The increased $CD8^+$ T-cell yield is desirable as clinical data indicate that an increased frequency of $CD8^+$ TIL infused was associated with tumor regression.[3] We performed additional multicolor flow cytometry analysis on post-REP melanoma TIL from a number of patients expanded with both platforms for 14 days. Panels were established to study the expression of differentiation, activation, and coinhibitory markers on T cells on the basis of expression of CD8, CD56, CD45RA, CD127, CD28, CD27, CCR7, BTLA, TIM3, and PD1. We focused on $CD8^+$ T cells, given its association with clinical response in our TIL clinical trial and also because of the presence of 4-BBL on the aAPC, which activates costimulation through 4-1BB mainly expressed on activated $CD8^+$ T cells. Costaining for CD45RA and CCR7 revealed that the majority of expanded $CD8^+$ cells with either protocol were $CD45RA^-CCR7^-$ as well as $CD127^-$, consistent with an effector-memory phenotype (Fig. 2A and data not shown).[21] CD27 and CD28 are other markers used to identify effector-memory cells. Although we did not find any differences in the frequency of $CD27^+$ cells emerging from the 2 expansion approaches, we observed a decreased frequency of $CD28^+$ T cells cocultured with aAPC (Fig. 2B; $P = 0.004$). This prompted us to examine the expression of inhibitory molecules such as TIM3, PD1, and BTLA. There was no significant difference in the expression of TIM3 on T cells propagated using the 2 protocols; however, PD1 was expressed on a lower percentage of $CD8^+$ T cells expanded with aAPC than with PBMC feeders (Fig. 2C; $P = 0.0394$). We also observed higher percentage of $CD8^+$ T cells expressing BTLA after aAPC REP compared with traditional REP (Fig. 2D; $P = 0.0435$). This was of great interest given our previous observation linking BTLA expression on $CD8^+$ TIL with clinical response after TIL infusion.[3] To further evaluate the activation status, we assessed expression of CD56 on $CD8^+$ TIL rapidly expanded with aAPC compared with PBMC feeders (Fig. 2D; $P = 0.0045$).[22,23] In summary, these flow cytometry data indicate that $CD8^+$ T cells propagated with the aAPC exhibit an effector-memory phenotype similar to the one generated with the feeders REP.

Gene Expression Reveals a Shared Effector and Stem-like Cell Profile in TIL Rapidly Expanded With aAPC

We profiled and compared gene expression using Affymetrix Human Gene ST 1.0 ST gene chip arrays (33,297 human transcripts) of 7 post-REP melanoma TIL lines rapidly expanded simultaneously with either the aAPC or PBMC feeders. The heat map presented in Figure 3A (left) shows the clustering of post-REP TIL depending on their expansion platform after removing the noise introduced by heterogeneity among patients. This source of variation remained lower than our point of comparison, which was the type of expansion platform (data not shown), validating the differentiation analysis. Using this approach, we found 26 highly significant genes ($P < 0.005$, 2-way analysis of variance based on cell line and expansion method) differentially downregulated or upregulated in the aAPC REP TIL (Fig. 3A, table). A more complete list of differentially expressed genes with a $P < 0.01$ cutoff for statistical significance is also shown in Table S1 (Supplemental Digital Content 2, http://links.lww.com/JIT/A353). Top differentially expressed genes in Figure 3A (table) included CD56 (NCAM1), which was the highest upregulated gene in the aAPC REP TIL, with a fold change of 2.78 ($P = 0.0004$). This result correlates with the protein expression previously observed by flow cytometry (Fig. 2D). The transcription factor FOXP3 was also upregulated 2.17-fold in TIL expanded with the aAPC platform. FOXP3 is usually associated with regulatory T cells (Tregs) but no other Treg-associated genes were found to be upregulated in the aAPC REP TIL in this assay. However, it must be noted that FOXP3 can also be expressed by recently activated conventional (non-Treg) T cells and IFN-γ producing nonregulatory T cells.[24,25] The most highly downmodulated gene was fibronectin-1 (FN1). Fibronectin, a multifunctional glycoprotein, is a major component of lymph nodes and participates in the CCR7/CCL21-mediated T-cell migration into the lymph node.[26,27] Although CD28 was not among the altered genes found after applying a more stringent *P*-value cutoff (Fig. 3A, table), it was significantly downmodulated in the aAPC REP TIL by −2.24-fold ($P = 0.0066$) (Table S1, Supplemental Digital Content 2, http://links.lww.com/JIT/A353). Similarly, the BTLA gene was upregulated +1.33-fold ($P = 0.0088$) (Table S1, Supplemental Digital Content 2, http://links.lww.com/JIT/A353). Both these results are in agreement with the flow cytometry data (Fig. 2C).

With the use of the ingenuity pathway analysis, we further analyzed the microarray data by undertaking a

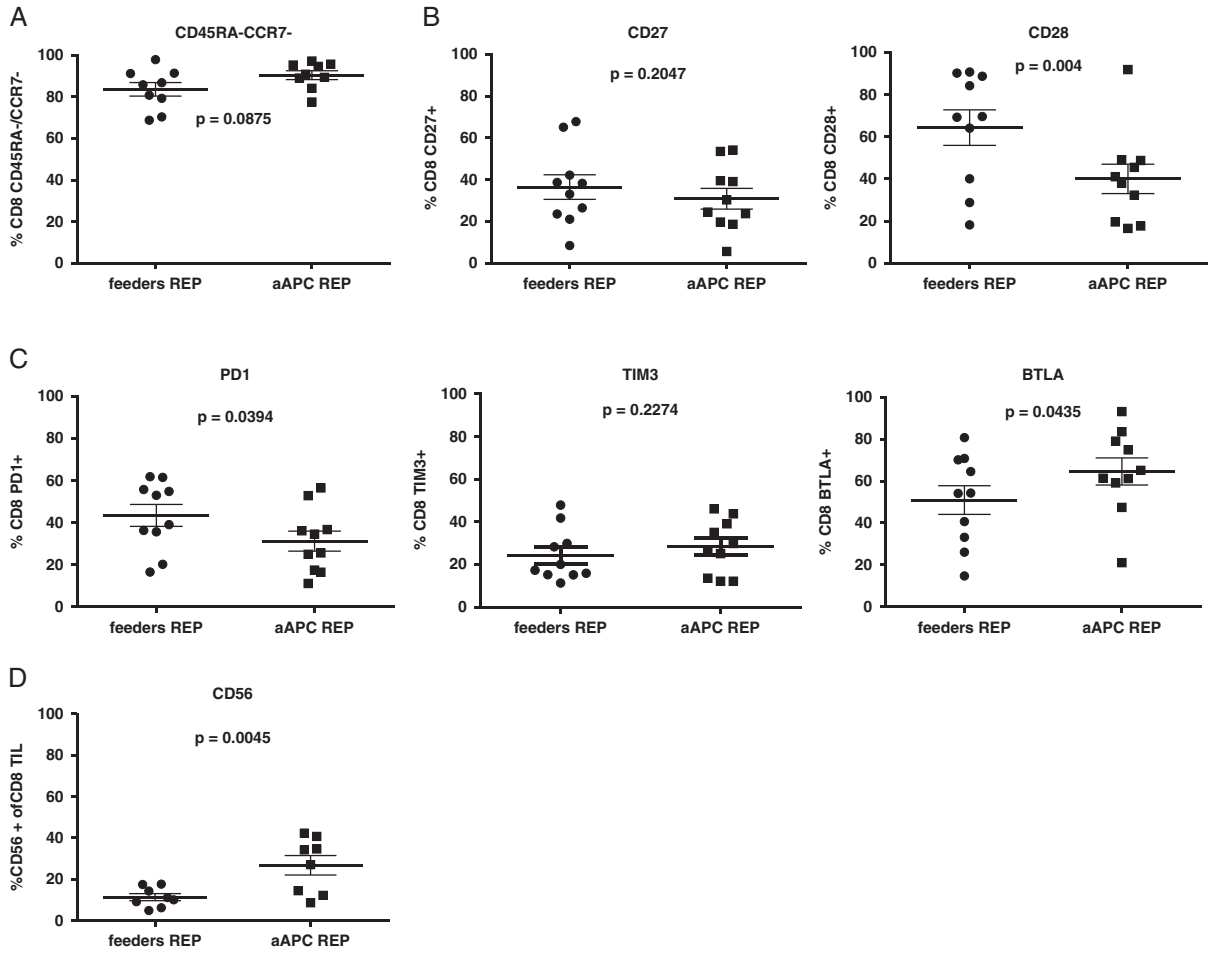

FIGURE 2. Intensive phenotyping by flow cytometry shows similarity in differentiation markers on post-REP CD8$^+$ TIL for both conditions with the exception of CD28, BTLA, and CD56. Post-REP TILs were stained with anti-CD3, anti-CD8, anti-CD4, anti-CD16, anti-CD56, anti-CD127, anti-CD28, anti-CD27, anti-CCR7, anti-BTLA, anti-TIM3, and anti-PD1. Results are shown after excluding dead cells by using Aqua live/dead (AQUA) staining. Graphs show 10 TIL lines, with only the most predominant markers presented. A, Frequency of CCR7$^-$CD45RA$^-$ in the CD8$^+$ T-cell population after expansion. B, Analysis of CD27 and CD28 expression in the CD8$^+$ T-cell population. C, Frequency of PD1-positive (left), TIM3-positive (middle), and BTLA-positive (right) cells in the CD8 population. D, Percentage of CD56$^+$ cells expended among the post-REP CD8$^+$ TILs. Gating was performed with the use of "fluorescence minus one (FMO)" controls. Statistics were determined using paired *t* test, and a *P* value <0.05 was considered significant.

pathway and network analysis (Fig. 3B). The pathways altered in the aAPC TIL with the lowest *P*-values were involved in stem cell or stem cell–associated pathways such as the Wnt pathway (see first 4 significant pathways on the left side of Fig. 3B). For the most part, these canonical pathways are not traditionally associated with lymphocyte development, but their involvement in pluripotency and differentiation of stem cells from nonlymphoid origins is intriguing.

Diversity of TCR Usage was Preserved in TIL Propagated With the aAPC Platform

TILs contain a diverse repertoire of T cells and the maintenance of this diversity as well as their ability to recognize multiple tumor-associated antigens is considered an advantage of TIL versus other forms of T-cell therapy.[28,29] Therefore, we compared the ability of the 2 approaches at rapidly expanding TIL on the overall TCR gene diversity of the post-REP products. We assessed the diversity and abundance of TCR expression by DTEA assay, a nonenzymatic assay based on bar-coded probes.[19] DTEA revealed that the abundance of the 45 Vα and 46 Vβ TCR chains was similar in both approaches (Fig. 4).

Post-REP TILs Expanded With aAPC Display Comparable Antitumor CTL Activity as TILs Expanded With the Conventional Feeders REP

We first assessed the cytolytic potential of both post-REP products by flow cytometry staining for intracellular cytotoxic granule proteins granzyme B and perforin. As shown in Figure 5A, no difference was found when TIL lines were rapidly expanded with either method. In addition, we measured tumor-specific CTL activity in post-REP TIL using a flow cytometry-based CTL assay staining for the extent of caspase 3 cleavage in melanoma cell line targets. In both cases, similar levels of HLA-restricted tumor cell killing were observed after the REP (Fig. 5B). Addition of anti-HLA-class I blocking antibodies to this assay inhibited caspase 3 cleavage, showing the specificity of the

A

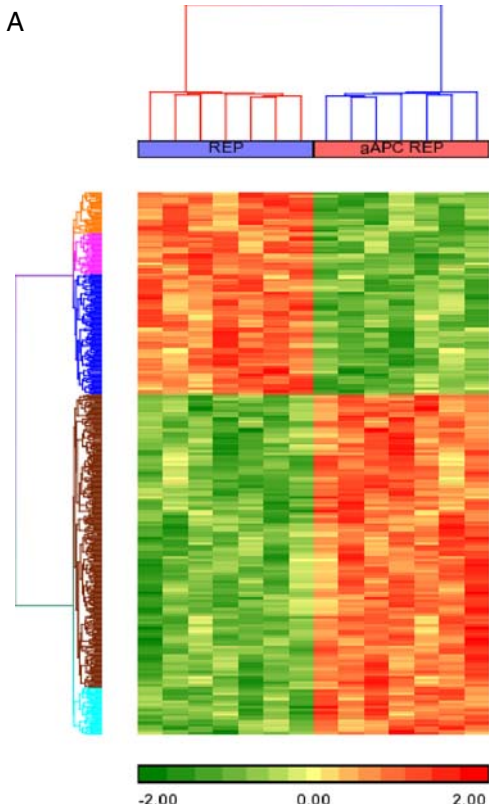

List of down-regulated and up-regulated genes in TIL rapidly expanded with aAPC (p< 0.005)

Gene Symbole	RefSeq	p-value	Fold-Change (aAPC REP vs. REP)
FN1	NM_212482	0.0045	-2.35
DENNDSA	NM_015213	0.0011	-1.93
GPR183	NM_004951	0.0030	-1.86
PEXSL	NM_016559	0.0033	-1.68
PIAS2	NM_004671	0.0027	-1.58
ADCY9	NM_001116	0.0030	-1.54
SGK3	NM_013257	0.0039	-1.52
CD200R1	NM_138806	0.0033	-1.51
KRT81	NM_002281	0.0037	1.51
CAMK1	NM_003656	0.0043	1.59
IPCEF1	NM_001130700	0.0044	1.59
PELO	NM_015946	0.0008	1.63
LZTFL1	NM_020347	0.0031	1.67
SLC4A10	NM_001178015	0.0036	1.76
ABTB2	NM_145804	0.0008	1.76
FCRL6	NM_001004310	0.0012	1.79
NRIP1	NM_003489	0.0011	1.79
SLC16A10	NM_018593	0.0034	1.93
TP73	NM_001126240	0.0003	1.93
IGF1	NM_001111283	0.0009	2.00
FOXP3	NM_014009	0.0011	2.17
RASSF4	NM_032023	0.0021	2.21
IKZF2	NM_016260	0.0003	2.24
AFAP1L2	NM_001001936	0.0039	2.42
DOK5	NM_018431	0.0032	2.52
NCAM1	NM_181351	0.0004	2.78

B

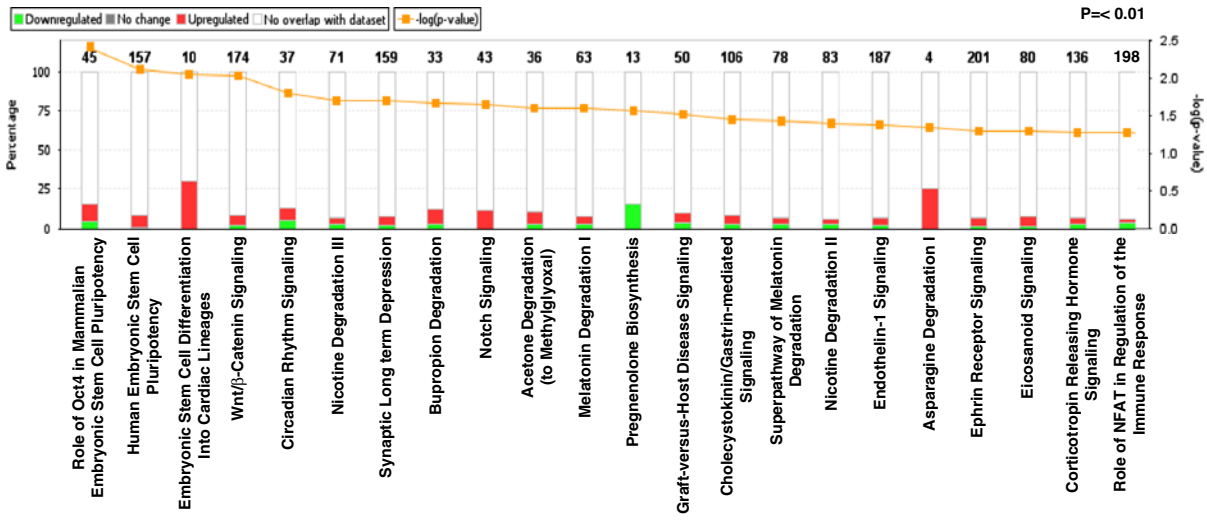

FIGURE 3. TIL rapidly expanded using the aAPC platform demonstrated a dual gene signature with attributes of effector and stem cells. A, Enrichment analysis of a global set of genes from post-REP TIL expanded with feeders or aAPC. The left shows a heat map cluster after removal of the cell line factor. On the right, a table presenting the top 26 genes, ranked by fold-expression changes with a *P* value <0.005, that are showing a differentiation of expression in aAPC post-REP TIL. A 2-way analysis of variance was performed using 2 parameters: cell line and expansion method. A comprehensive list of genes ranked by enrichment scores are shown in Table S1 (Supplemental Digital Content 2, http://links.lww.com/JIT/A353). B, Graph showing the percentage (and the number in bold) of gene upregulated (red columns) and downregulated (green columns) in the different canonical pathways. The dark yellow line (log) shows the intensity of change in the gene expression. Analysis was performed using the "ingenuity pathway analysis (IPA)" ($P < 0.01$).

TIL in each case. We also measured IFN-γ release in response to coincubation of post-REP TIL with HLA-matched melanoma cells and found similar IFN-γ secretion capacities of the post-REP TIL in both cases (Fig. 5C).

Application of aAPC for Rapid Expansion of Melanoma TIL Using the G-REX System

Currently, our group at MDACC has adopted the use of the G-REX culture flask system (Wilson-Wolf,

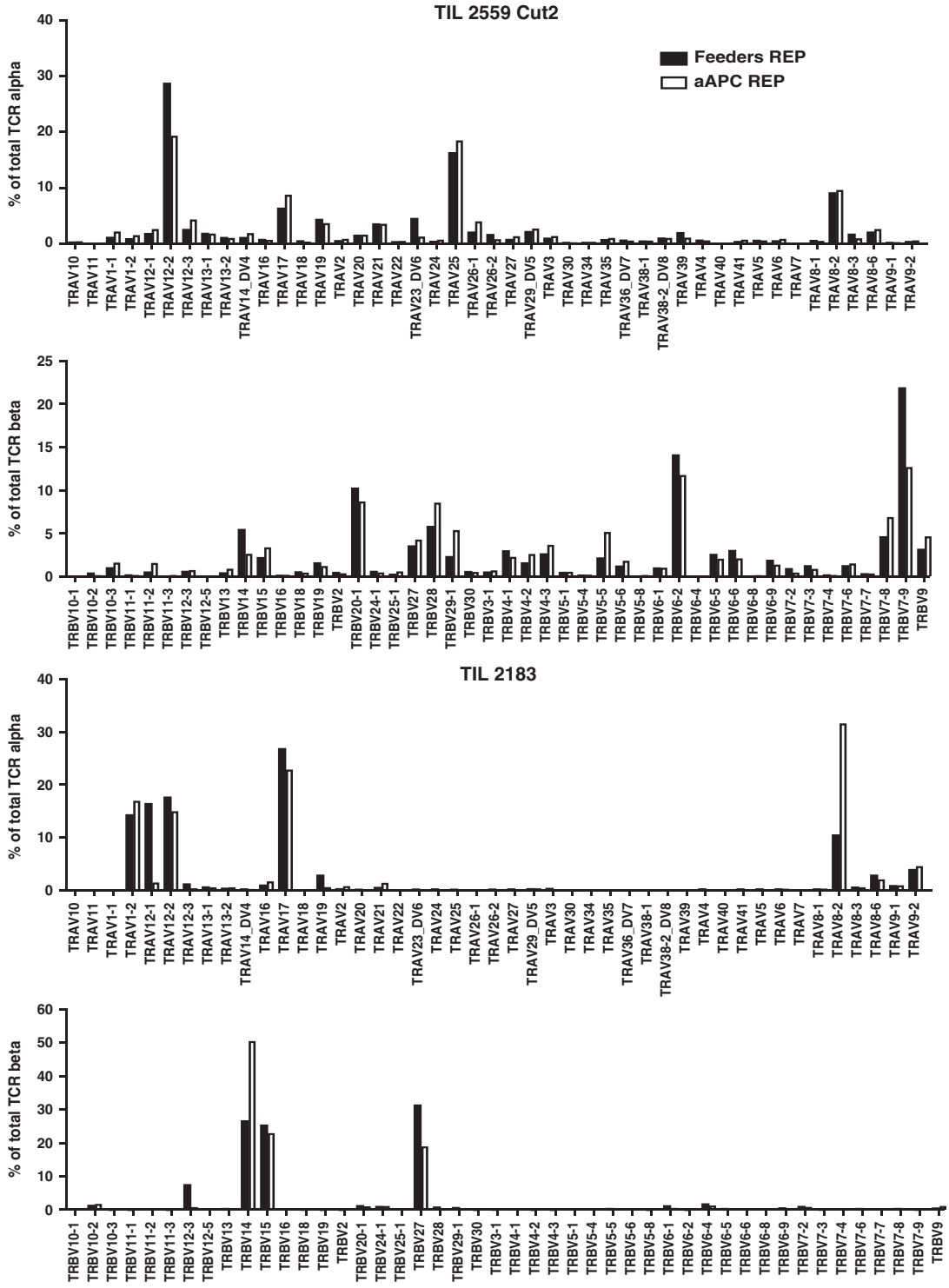

FIGURE 4. aAPC REP does not favor or disfavor expansion of predominant melanoma TIL clonotypes. Measurement of the expression of major TCR α and β chain gene usage found after rapid expansion (REP) with either aAPC REP or PBMC feeders using the NanoString NCounter technology. This assay directly digitally reads out the level of expression of 45 possible Vα and all known 46 Vβ genes in RNA isolates using bar-coded probes. Two examples representative of 6 TIL lines from 6 melanoma patients.

Minneapolis, MN) for the clinical-grade REP of melanoma TIL for patient therapy. This G-REX system uses flasks that have a gas permeable membrane at the bottom of the flask where cells sit during culture allowing gas exchange directly through this membrane rather than needing to diffuse through the culture medium on top of the cells.[16,30] We have adopted the G-REX 100 M flask system having a 100 cm^2 gas permeable membrane for the clinical-grade

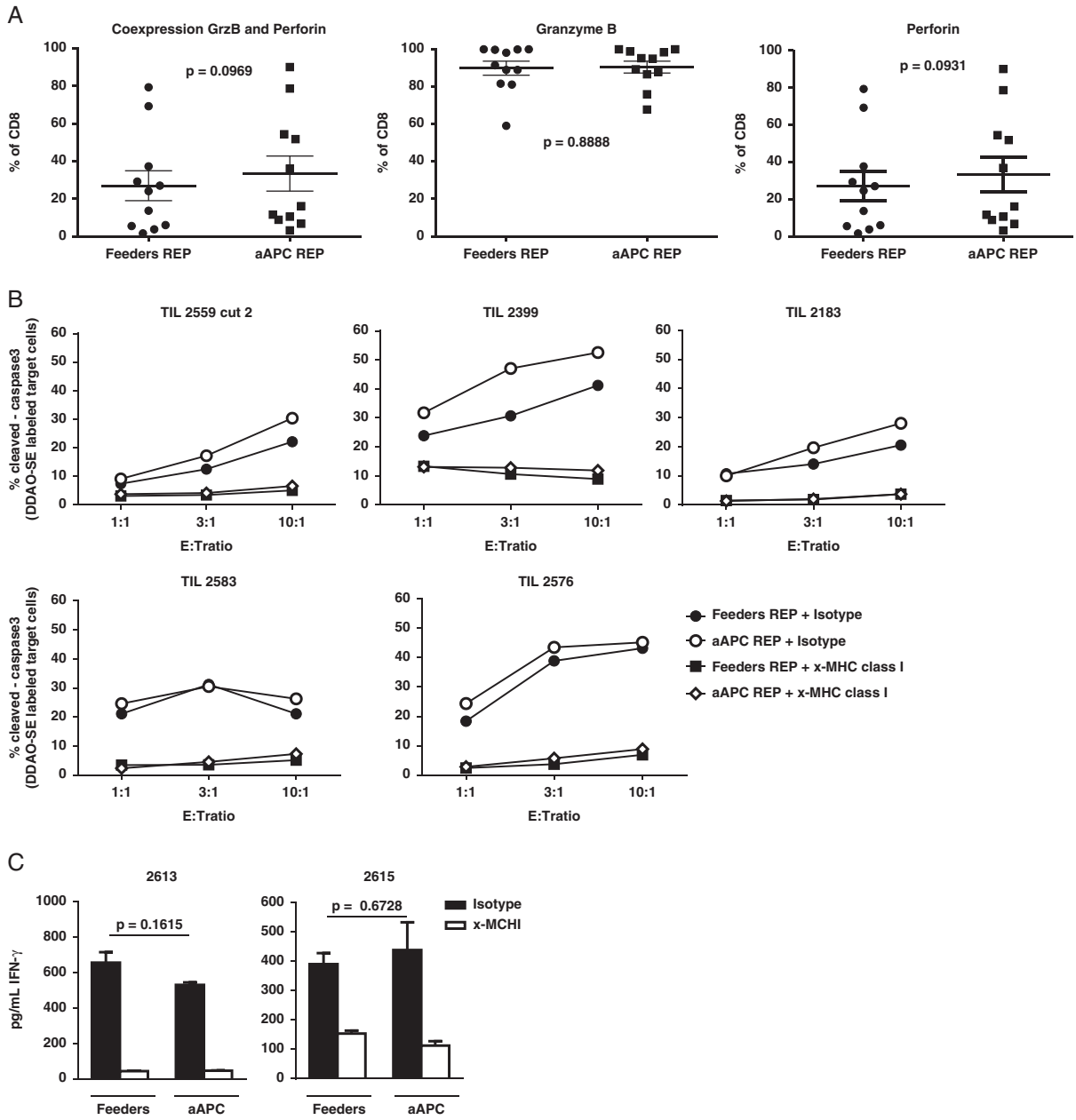

FIGURE 5. Melanoma CD8$^+$ TIL rapidly expanded with the aAPC platform demonstrated an antitumor potential equivalent than TIL expanded with PBMC feeders. A, On day 14 of the REP, cells were harvested, permeabilized, and stained for surface CD8, AQUA, and intracellular granzyme B and perforin. B, Post-REP TILs were cocultured with DDAO-SE labeled autologous or HLA-A-matched tumor cell line for 3 hours. Tumor cells were preincubated with 80 μg/mL of blocking antibodies specific for MHC-I (clone W6/32) as a test for class I dependency of killing or the corresponding isotype (IgG2a). Target-to-effector (T:E) ratios of 1:1, 1:3, and 1:10 were used. After 3 hours, cells were permeabilized and stained for active caspase-3 by flow cytometry. The graphs indicate percent expression of active caspase-3 in the tumor cells. The MHC-1 blocking control is shown on the bottom row. C, Post-REP TILs and tumor cells were cocultured with or without MHC-I blocking antibody for 16 hours at a ratio of 1:1. Supernatant was collected and an IFN-γ ELISA assay was performed in triplicates and the mean ± SE is shown for each. Statistics were determined using paired *t* test, and a *P* value < 0.05 was considered significant.

rapid expansion of melanoma TIL in our phase II clinical trials using the PBMC feeder system. Here, we wanted to also test how the aAPCs support the rapid expansion of melanoma TIL with the help of this new G-REX system using the same aAPC to TIL (50:1) and PBMC feeder to TIL (200:1) ratios as before. We compared the propagation of 12 different melanoma pre-REP TIL lines and did post-REP phenotyping by flow cytometry using the same antibody panels used before. As shown in Figure 6A, no differences in fold expansion were observed when TILs were rapidly expanded with the aAPC or with the PBMC feeders in the G-REX 100 M flask. We observed a high fold expansion rate with the use of the G-REX 100 M for both REP conditions (Fig. 6A).

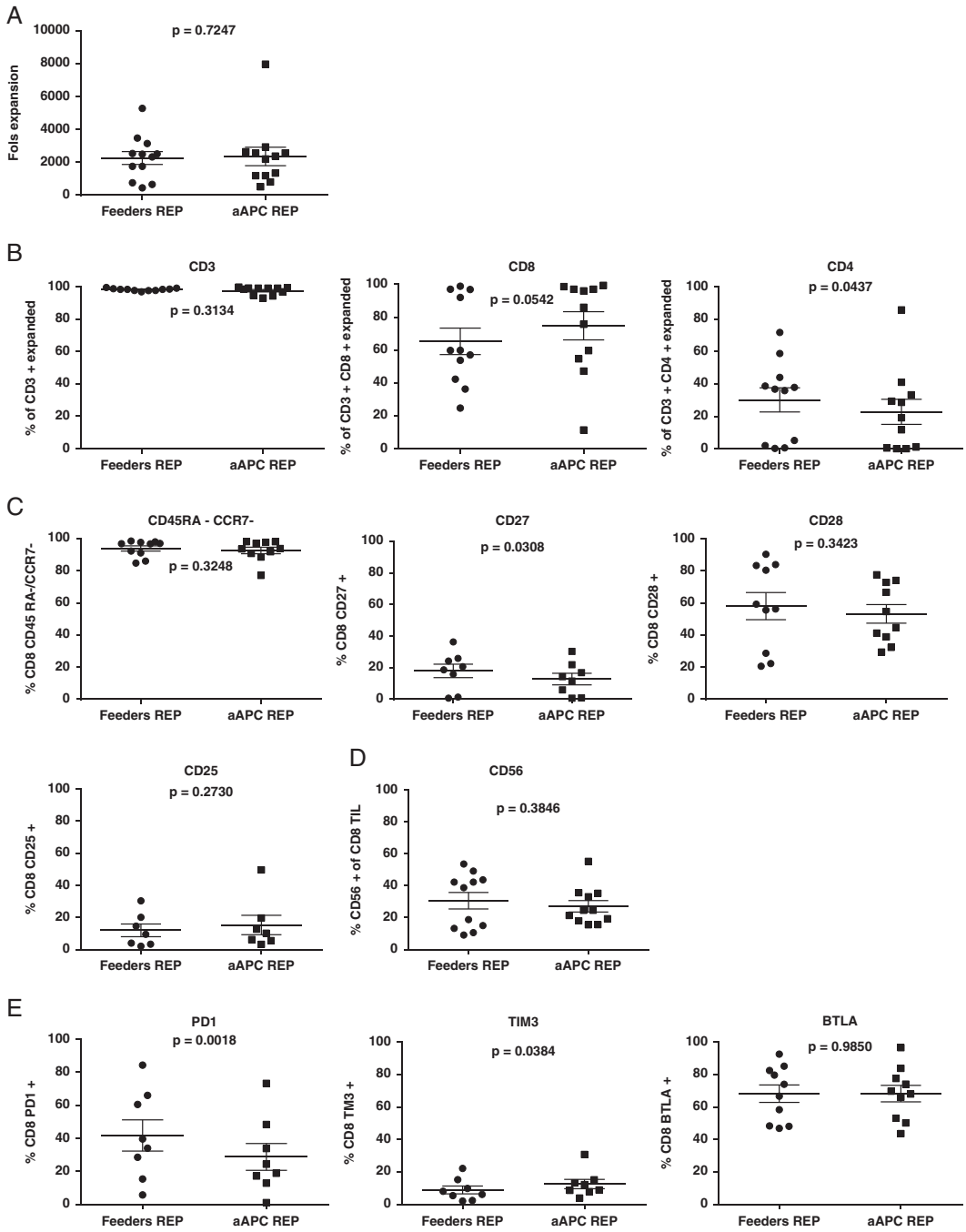

FIGURE 6. Melanoma TILs rapidly expanded with the aAPC in the G-REX flask have a comparable phenotype when expanded with the PBMC feeders. Flow cytometry on post-REP CD8$^+$ TIL for both conditions shows similarity in differentiation, activation, and inhibition molecules. Post-REP TILs were stained with anti-CD3, anti-CD8, anti-CD4, anti-CD16, anti-CD56, anti-CD127, anti-CD28, anti-CD27, anti-CCR7, anti-CD25, anti-BTLA, anti-TIM3, and anti-PD1. Results are shown after excluding dead cells by using Aqua live/dead (AQUA) staining. Graphs show 10 TIL lines expanded in the G-REX flask. A, Graph showing cumulative data of fold expansion of bulk TIL lines. B, Percentage of CD3$^+$ TIL post-REP (left graph) obtained after 14 days of expansion. Middle and right graphs show post-REP frequency of, respectively, CD3$^+$CD8$^+$ and CD3$^+$CD4$^+$ TIL. Frequency of CCR7$^-$CD45RA$^-$ in the CD8$^+$ T-cell population after expansion. C, Frequency of CCR7$^-$CD45RA$^-$ (upper left graph), CD27 (middle), CD28 (right), and CD25 (lower left graph) in the CD8$^+$ T-cell population after expansion. Frequency of PD1-positive, TIM3-positive, and BTLA-positive cells in the CD8 population. D, Percentage of CD56$^+$ cells expended among the post-REP CD8$^+$ TIL. E, Frequency of PD1-positive (left), TIM3-positive (middle), and BTLA-positive (right) cells in the CD8 population. Gating was performed with the use of "fluorescence minus one (FMO)" controls. Statistics were determined using paired *t* test, and a *P* value < 0.05 was considered significant.

As shown in Figure 6B (left graph), the post-REP product from the G-REX system mostly constituted $CD3^+$ cells for both conditions. Similar frequencies of $CD8^+$ TIL were obtained, except that the aAPC REP condition tended to yield a higher $CD8^+$ cell frequency, although this did not reach statistical significance ($P = 0.0542$; Fig. 6B). $CD4^+$ T-cell frequency was, however, significantly lower in the aAPC G-REX 100 M REP cultures (Fig. 6B, far right panel).

No major differences in the $CD45RA^-CCR7^-$ subset, CD25, and CD27 expressions were found (Fig. 6C, middle graph). In addition, CD28 expression showed no significant difference between aAPC and PBMC feeders REP in the G-REX 100 M flask (Fig. 6C, right graph). The frequency of $CD3^+CD8^+CD56^+$ cells was also similar between the aAPC and PBMC feeders REP (Fig. 6D). The frequency of cells with a late-stage $CD8^+$ cytotoxic T-cell phenotype based on expression of markers such as CD56 and CD57 ($CD28^-CD56^+$ or $CD28^-CD57^+$) was low but favored the aAPC protocol regarding a lower $CD28^-CD57^+$ population, suggesting that most of the expanded $CD8^+$ cells were activated effector-memory cells (Fig. S2, Supplemental Digital Content 3, http://links.lww.com/JIT/A354).

As before, we also measured the expression of PD1, TIM3, and BTLA on the post-REP cells. No significant differences were found in the frequencies of $CD8^+BTLA^+$ cells with aAPC versus PBMC feeders in the G-REX system (Fig. 6E). However, the frequency of $PD1^+$ $CD8^+$ cells was significantly lower when TILs were rapidly expanded with the aAPC in the G-REX flask and the frequency of TIM3-expressing cells was slightly higher under the aAPC condition (Fig. 6E, left panel), although lower than what we observed in the regular flask system before.

DISCUSSION

ACT of autologous TIL has been one of the most effective treatments for refractory metastatic melanoma with clinical response rates close to 50%.[1–3] However, only a few cancer centers are currently capable of performing this therapy because of the intricate culture steps, making its implementation in a broader number of institutions challenging. One of the main obstacles is the technical complexity of expanding TIL to the large numbers needed to achieve clinical effectiveness (20–150 billion). The need to procure large numbers of donor-derived pooled PBMC cell products as "feeders" to provide cell support for the TIL REP represents both a technical and financial problem. The rapid expansion usually requires a 200:1 PBMC feeders to TIL ratio to facilitate optimal TIL growth, especially of $CD8^+$ T cells, which are critical for mediating antitumor activity. In addition, procurement of PBMC feeder products introduces logistics issues with the collection of donor apheresis products, batch-to-batch variability, and increased costs. The results presented here indicate that the use of a genetically modified antigen-presenting cell line based on the K562 erythroleukemia cell line can be a practical and effective alternative to PBMC feeders for TIL rapid expansion. Using the K562 clone 4, we developed an optimal and clinically translatable approach that can rapidly expand melanoma TIL at comparable rates of expansion as the PBMC feeders REP generating a final product that is phenotypically and functionally similar.

We tested different aAPC:TIL ratios and found that an aAPC:TIL ratio of 50:1 was ideal in that it facilitated optimal rates of expansion comparable to the PBMC feeders REP while still maintaining an aAPC:TIL ratio that was well below the 200:1 PBMC feeder:TIL ratio used in the conventional REP. We were able to induce even higher rates of expansion (> 2000-fold) when the aAPCs were used in the G-REX flask system without having to restimulate the TIL during the expansion phase. This was achieved with only one initial stimulation using the aAPC compared with previous studies using a lower 2:1 aAPC:TIL ratio in which an additional round of stimulation was needed to increase the fold expansion to levels achieved here.[31] We also observed that our aAPC favored the proliferation of the $CD8^+$ TIL over $CD4^+$ cells. This higher percentage of $CD8^+$ T cells in the final REP product may be attributed to enhanced 4-1BB costimulation provided to the activated TIL by the 4-1BBL on the surface of aAPC, which was previously described to preferentially expand $CD8^+$ T cells.[32] In fact, 4-1BBL was reported to be essential to expand TIL directly from single cell suspension of tumor digests using K562-aAPC and IL-2, with favored expansion toward $CD8^+$ T cells but also NK cells given the absence of CD3 stimulation in this study.[33] Moreover, our group previously demonstrated that engagement of 4-1BB during the initial phase of the REP favors expansion of $CD8^+$ T cells among TILs.[34]

Given our previous report correlating a higher frequency and number of infused $CD8^+$ T cells with clinical response in the first 31 patients of our TIL therapy trial at MDACC,[3] we decided to further characterize the post-REP $CD8^+$ T cells by measuring the expression of a number of lineage-specific markers, as well as activation, differentiation, and negative costimulatory molecules and differential gene expression analysis using gene chips on the final TIL products. One of the major differences we observed was a higher percentage of $CD8^+$ TIL positive for the expression of NCAM (CD56) in the aAPC REP compared with the PBMC feeders REP. Expression of CD56 by $CD8^+$ T cells is usually associated with a highly cytotoxic profile and increased effector cell differentiation.[22,23] It has been previously reported that stimulation with 4-1BBL can enhance the killing potential of $CD3^+CD56^+$ cells and also of $CD8^+$ T cells, but to our knowledge, expression of CD56 on $CD8^+$ T cells induced by 4-1BB stimulation was not investigated.[35,36] The increased frequency of $CD8^+CD56^+$ cells in the post-REP product generated with the aAPC in regular T-25 flasks could also indicate a more differentiated effector-memory phenotype as the frequency of $CD8^+CD28^+$ cells also tended to be lower. CD56 expression was also found on terminally differentiated T cells, but these cells were also expressing CD45RA and high levels of PD1, which is not the case in our study.[37,38] It is also possible that decreased CD28 is reversible and due to the high CD86 expression on the aAPC that may downmodulate, but not permanently eliminate, CD28 expression. Previous published data from patients treated with tumor-specific T cells have also found that activated T cells can the reexpress CD28 and CD27 in vivo after adoptive transfer.[39] However, the decreased CD28 expression in the T-flask system with the aAPC was not observed when TILs were rapidly expanded using the G-REX flasks, which we are now using for clinical-grade TIL expansion in our ACT trials. Thus, the data from our G-REX flask system indicated that CD28 expression can be preserved with the aAPC REP.

It is interesting to note that the difference with the CD56 expression between the 2 expansion platforms was

also lost in the G-REX flask and similar frequencies of $CD45RA^{-}CCR7^{-}$ cells were observed, independently of the device that was used for the REP. Thus, the use of the G-REX flask to rapidly expand TIL seems to have a bigger effect on the phenotype of the expanded TIL when using PBMC feeders in the REP, whereas the phenotype of the TIL seems to be more stable with the aAPC REP independently of the type of flask. It is possible that the improved gas exchange in the G-REX flasks (increased O_2 availability and faster CO_2 diffusion) due to the nature of this culture system versus the tradition T-flask may alter the metabolism of the cells.

Our microarray gene expression analysis suggests that the aAPC may not indeed lead to increased T-cell differentiation. Pathway analysis conducted on the 7 TIL lines rapidly expanded with either the PBMC feeders or the aAPC platform after microarray analysis demonstrated upregulation of genes belonging to canonical pathways such as the Wnt pathway and other stem cell pathways. Recently, Lee et al,[40] reported that induction of 4-1BB signaling leads indirectly to activation of the TCF-1/β-catenin pathway in T cells, which involved activation of the Wnt signaling pathway downstream of 4-1BB. This observation was attributed to a delayed effect of 4-1BB signaling and was visible 1 to 2 days after 4-1BB ligation but was not investigated at later time points. The upregulation of genes belonging to such pathway could confer a better persistence potential to cells harboring a more activated and cytotoxic phenotype, which are not thought to persist long after adoptive transfer. Nonetheless, once this aAPC platform is translated into clinic, long-term blood tracking of TIL T-cell clones after infusion will be required to determine any beneficial effects on TIL persistence and whether any of these differentially expressed genes correlate with differences in clinical response.

In addition to the upregulation of genes belonging to different stem cell pathways, the differential gene expression profiling found increased expression of some unexpected genes. The transcription factor FOXP3 was surprising, given that no other genes attributed to a Treg signature were overexpressed in TIL expanded with the aAPC. So far, other than FOXP3 being a maker for T-cell activation, no other conclusion can be currently drawn.[24] Insulin growth factor-1 (IGF-1), an endocrine mediator of growth and development, was also one of the most upregulated genes in TIL expanded with aAPC compared with the feeder platform. IGF-1 was reported to be implicated in T-cell differentiation in the thymus as well as NK cell development and cytotoxic function.[41,42] One of the major genes found to be downregulated in post-aAPC REP TIL was one of the 3 modules that constitutes fibronectin, FN1. FN1 is implicated in wound healing, and high levels of this molecule were reported in IL-10 producer type 2 tumor-infiltrating macrophages, correlating with reduced survival in renal cancer.[43,44] Increased level of fibronectin in the serum has also been linked with a lack of clinical response to high-dose IL-2 therapy in melanoma and renal cell cancer patients.[45] Literature linking FN1 and lymphocytes is mostly about expression of fibronectin following T-cell activation (4–7 d later), but not precisely on the FN1 constituent.[46,47] As this constituent has been associated with immune-suppression and wound healing, its downregulation in TIL expanded with aAPC compared with those amplified with feeders could be seen as a positive asset.

One of the major strengths of ACT with TIL is that the infusion product still retains a reasonable diverse T-cell repertoire generating specificity against multiple known and unknown tumor antigens.[48] Some antigens are derived from self/mutated protein, whereas others are not yet identified.[28,29] Targeting multiple tumor antigens simultaneously gives a strong advantage toward avoiding tumor escape due to antigen loss. This was a major point in our study, as we wanted to make sure that we were preserving an equivalent clonal diversity in comparison with the infusion product obtained by using the PBMC feeder platform. To do this we compared the clonal diversity generated with both platforms using the DTEA method to assess for expression of Vα and Vβ TCR and saw the preservation of the same array of different TCR α and β genes in post-REP TIL expanded using both methods. Furthermore, the antitumor CTL function of post-aAPC REP TIL against autologous or HLA-A-matched tumor targets was as efficient as the one observed with the TIL rapidly expanded using the conventional method. This was consistent with a similar level of intracytoplasmic cytotoxic granule protein content (granzyme B/perforin expression by flow cytometry).

In conclusion, our study has demonstrated significant expansion of melanoma TIL using genetically modified K562 as aAPC. Melanoma TIL can be comparably expanded with aAPC as with the PBMC feeders REP yielding cells with similar phenotypic and effector functional profiles as well as similar TCR gene diversity. However, some interesting differences were noted particularly in the gene expression profiles indicating that the aAPC REP may yield cells with a different functional phenotype in vivo after adoptive transfer. Thus, this will be determined in clinical trial with evaluation of clinical responses and long-term persistence tracking of the infused cells.

ACKNOWLEDGMENTS

The authors would like to thank the MDACC TIL laboratory members: Rahmatu Mansaray, Orenthial J. Fulbright, Renjith Ramachandran, Seth Wardell, Audrey Gonzalez, and Valentina Dumitru. The authors would also like to thank all the additional clinical and research staff in the Melanoma Medical Oncology Department as well as the Division of Pediatrics at the MDACC that contributed to this study.

CONFLICTS OF INTEREST/ FINANCIAL DISCLOSURES

Supported by the CPRIT grant (RP110553-P4) and Marie-Andrée Forget thanks CPRIT for her salary support. The authors would also like to acknowledge the support provided by the Adelson Medical Research Foundation (AMRF), and the Mulva Foundation as well as the National Institute of Health (NIH) Melanoma SPORE (P50 CA093459-08) and the R01 CA116206-09.

All authors have declared there are no financial conflicts of interest with regard to this work.

REFERENCES

1. Dudley ME, Wunderlich JR, Yang JC, et al. Adoptive cell transfer therapy following non-myeloablative but lymphodepleting chemotherapy for the treatment of patients with refractory metastatic melanoma. *J Clin Oncol.* 2005;23:2346–2357.
2. Besser MJ, Shapira-Frommer R, Treves AJ, et al. Clinical responses in a phase II study using adoptive transfer of short-term cultured tumor infiltration lymphocytes in metastatic melanoma patients. *Clin Cancer Res.* 2010;16:2646–2655.

3. Radvanyi LG, Bernatchez C, Zhang M, et al. Specific lymphocyte subsets predict response to adoptive cell therapy using expanded autologous tumor-infiltrating lymphocytes in metastatic melanoma patients. *Clin Cancer Res*. 2012;18:6758–6770.
4. Rosenberg SA, Yang JC, Sherry RM, et al. Durable complete responses in heavily pretreated patients with metastatic melanoma using T-cell transfer immunotherapy. *Clin Cancer Res*. 2011;17:4550–4557.
5. Itzhaki O, Hovav E, Ziporen Y, et al. Establishment and large-scale expansion of minimally cultured "young" tumor infiltrating lymphocytes for adoptive transfer therapy. *J Immunother*. 2011;34:212–220.
6. Pilon-Thomas S, Kuhn L, Ellwanger S, et al. Efficacy of adoptive cell transfer of tumor-infiltrating lymphocytes after lymphopenia induction for metastatic melanoma. *J Immunother*. 2012;35:615–620.
7. Riddell SR, Watanabe KS, Goodrich JM, et al. Restoration of viral immunity in immunodeficient humans by the adoptive transfer of T cell clones. *Science*. 1992;257:238–241.
8. Dudley ME, Rosenberg SA. Adoptive-cell-transfer therapy for the treatment of patients with cancer. *Nat Rev Cancer*. 2003;3:666–675.
9. Dudley ME, Wunderlich JR, Shelton TE, et al. Generation of tumor-infiltrating lymphocyte cultures for use in adoptive transfer therapy for melanoma patients. *J Immunother*. 2003;26:332–342.
10. Lozzio CB, Lozzio BB. Human chronic myelogenous leukemia cell-line with positive Philadelphia chromosome. *Blood*. 1975;45:321–334.
11. Maus MV, Thomas AK, Leonard DG, et al. Ex vivo expansion of polyclonal and antigen-specific cytotoxic T lymphocytes by artificial APCs expressing ligands for the T-cell receptor, CD28 and 4-1BB. *Nat Biotechnol*. 2002;20:143–148.
12. Denis-Mize KS, Dupuis M, MacKichan ML, et al. Plasmid DNA adsorbed onto cationic microparticles mediates target gene expression and antigen presentation by dendritic cells. *Gene Ther*. 2000;7:2105–2112.
13. Singh H, Figliola MJ, Dawson MJ, et al. Reprogramming CD19-specific T cells with IL-21 signaling can improve adoptive immunotherapy of B-lineage malignancies. *Cancer Res*. 2011;71:3516–3527.
14. Butler MO, Lee JS, Ansen S, et al. Long-lived antitumor $CD8^+$ lymphocytes for adoptive therapy generated using an artificial antigen-presenting cell. *Clin Cancer Res*. 2007;13:1857–1867.
15. Manuri PV, Wilson MH, Maiti SN, et al. piggyBac transposon/transposase system to generate CD19-specific T cells for the treatment of B-lineage malignancies. *Hum Gene Ther*. 2010;21:427–437.
16. Vera JF, Brenner LJ, Gerdemann U, et al. Accelerated production of antigen-specific T cells for preclinical and clinical applications using gas-permeable rapid expansion cultureware (G-Rex). *J Immunother*. 2010;33:305–315.
17. Li Y, Liu S, Hernandez J, et al. MART-1-specific melanoma tumor-infiltrating lymphocytes maintaining CD28 expression have improved survival and expansion capability following antigenic restimulation in vitro. *J Immunol*. 2010;184:452–465.
18. Singh H, Manuri PR, Olivares S, et al. Redirecting specificity of T-cell populations for CD19 using the Sleeping Beauty system. *Cancer Res*. 2008;68:2961–2971.
19. Zhang M, Maiti S, Bernatchez C, et al. A new approach to simultaneously quantify both TCR alpha- and beta-chain diversity after adoptive immunotherapy. *Clin Cancer Res*. 2012;18:4733–4742.
20. He L, Hakimi J, Salha D, et al. A sensitive flow cytometry-based cytotoxic T-lymphocyte assay through detection of cleaved caspase 3 in target cells. *J Immunol Methods*. 2005;304:43–59.
21. Romero P, Zippelius A, Kurth I, et al. Four functionnally distinct populations of human effector-memory $CD8^+$ T lymphocytes. *J Immunol*. 2007;178:4112–4119.
22. Satoh M, Seki S, Hashimoto W, et al. Cytotoxic gammadelta or alphabeta T cells with a natural killer cell marker, CD56, induced from human peripheral blood lymphocytes by a combination of IL-12 and IL-2. *J Immunol*. 1996;157:3886–3892.
23. Pittet MJ, Speiser DE, Valmori D, et al. Cutting edge: cytolytic effector function in human circulating $CD8^+$ T cells closely correlates with CD56 surface expression. *J Immunol*. 2000;164:1148–1152.
24. Miyara M, Yoshioka Y, Kitoh A, et al. Functional delineation and differentiation dynamics of human $CD4^+$ T cells expressing the FoxP3 transcription factor. *Immunity*. 2009;30:899–911.
25. Tran DQ, Ramsey H, Shevach EM. Induction of FOXP3 expression in naive human $CD4^+$FOXP3 T cells by T-cell receptor stimulation is transforming growth factor-beta dependent but does not confer a regulatory phenotype. *Blood*. 2007;110:2983–2990.
26. Kaldjian EP, Gretz JE, Anderson AO, et al. Spatial and molecular organization of lymph node T cell cortex: a labyrinthine cavity bounded by an epithelium-like monolayer of fibroblastic reticular cells anchored to basement membrane-like extracellular matrix. *Int Immunol*. 2001;13:1243–1253.
27. Shannon LA, Calloway PA, Welch TP, et al. CCR7/CCL21 migration on fibronectin is mediated by phospholipase Cgamma1 and ERK1/2 in primary T lymphocytes. *J Biol Chem*. 2010;285:38781–38787.
28. Kvistborg P, Shu CJ, Heemskerk B, et al. TIL therapy broadens the tumor-reactive $CD8^+$ T cell compartment in melanoma patients. *Oncoimmunology*. 2012;1:409–418.
29. Robbins PF, Lu YC, El-Gamil M, et al. Mining exomic sequencing data to identify mutated antigens recognized by adoptively transferred tumor-reactive T cells. *Nat Med*. 2013;19:747–752.
30. Jin J, Sabatino M, Somerville R, et al. Simplified method of the growth of human tumor infiltrating lymphocytes in gas-permeable flasks to numbers needed for patient treatment. *J Immunother*. 2012;35:283–292.
31. Ye Q, Loisiou M, Levine BL, et al. Engineered artificial antigen presenting cells facilitate direct and efficient expansion of tumor infiltrating lymphocytes. *J Trans Med*. 2011;9:131–143.
32. Shuford WW, Klussman K, Tritchler DD, et al. 4-1BB costimulatory signals preferentially induce $CD8^+$ T cell proliferation and lead to the amplification in vivo of cytotoxic T cell responses. *J Exp Med*. 1997;186:47–55.
33. Friedman KM, Devillier LE, Feldman SA, et al. Augmented lymphocyte expansion from solid tumors with engineered cells for costimulatory enhancement. *J Immunother*. 2011;34:651–661.
34. Chacon JA, Wu RC, Sukhumalchandra P, et al. Co-stimulation through 4-1BB/CD137 improves the expansion and function of $CD8^+$ melanoma tumor-infiltrating lymphocytes for adoptive T-cell therapy. *PLoS One*. 2013;8:e60031.
35. Zhu BQ, Ju SW, Shu YQ. CD137 enhances cytotoxicity of $CD3^+CD56^+$ cells and their capacities to induce $CD4^+$ Th1 responses. *Biomed Pharmacother*. 2009;63:509–516.
36. Hernandez-Chacon JA, Li Y, Wu RC, et al. Costimulation through the CD137/4-1BB pathway protects human melanoma tumor-infiltrating lymphocytes from activation-induced cell death and enhances antitumor effector function. *J Immunother*. 2011;34:236–250.
37. Franceschetti M, Pievani A, Borleri G, et al. Cytokine-induced killer cells are terminally differentiated activated CD8 cytotoxic T-EMRA lymphocytes. *Exp Hematol*. 2009;37:616–628, e612.
38. Legat A, Speiser DE, Pircher H, et al. Inhibitory receptor expression depends more dominantly on differentiation and activation than "exhaustion" of human CD8 T cells. *Front Immunol*. 2013;4:455–469.
39. Chapuis AG, Thompson JA, Margolin KA, et al. Transferred melanoma-specific $CD8^+$ T cells persist, mediate tumor regression, and acquire central memory phenotype. *Proc Natl Acad Sci USA*. 2012;109:4592–4597.

40. Lee DY, Choi BK, Lee DG, et al. 4-1BB signaling activates the T cell factor 1 effector/beta-catenin pathway with delayed kinetics via ERK signaling and delayed PI3K/AKT activation to promote the proliferation of $CD8^+$ T cells. *PLoS One*. 2013;8:e69677.
41. Kermani H, Goffinet L, Mottet M, et al. Expression of the growth hormone/insulin-like growth factor axis during Balb/c thymus ontogeny and effects of growth hormone upon ex vivo T cell differentiation. *Neuroimmunomodulation*. 2012;19:137–147.
42. Ni F, Sun R, Fu B, et al. IGF-1 promotes the development and cytotoxic activity of human NK cells. *Nat Commun*. 2013; 4:1479–1489.
43. Martinez FO, Gordon S, Locati M, et al. Transcriptional profiling of the human monocyte-to-macrophage differentiation and polarization: new molecules and patterns of gene expression. *J Immunol*. 2006;177:7303–7311.
44. Dannenmann SR, Thielicke J, Stockli M, et al. Tumor-associated macrophages subvert T-cell function and correlate with reduced survival in clear cell renal cell carcinoma. *Oncoimmunology*. 2013;2:e23562.
45. Sabatino M, Kim-Schulze S, Panelli MC, et al. Serum vascular endothelial growth factor and fibronectin predict clinical response to high-dose interleukin-2 therapy. *J Clin Oncol*. 2009;27:2645–2652.
46. Wagner C, Burger A, Radsak M, et al. Fibronectin synthesis by activated T lymphocytes: up-regulation of a surface-associated isoform with signalling function. *Immunology*. 2000;99:532–539.
47. Blum S, Hug F, Hansch GM, et al. Fibronectin on activated T lymphocytes is bound to gangliosides and is present in detergent insoluble microdomains. *Immunol Cell Biol*. 2005; 83:167–174.
48. Andersen RS, Thrue CA, Junker N, et al. Dissection of T-cell antigen specificity in human melanoma. *Cancer Res*. 2012; 72:1642–1650.

